Available online at www.sciencedirect.com
SCIENCE DIRECT®
International Journal of Engineering Science 44 (2006) 37–48
International Journal of Engineering Science
www.elsevier.com/locate/ijengsci

Analyzing the interaction between collinear interfacial cracks by an efficient boundary element-free method

Yuzhou Sun [a], Zan Zhang [b], S. Kitipornchai [a], K.M. Liew [a,*]

[a] Department of Building and Construction, City University of Hong Kong, Tat Chee Avenue, Kowloon, Hong Kong
[b] Shanghai Institute of Applied Mathematics and Mechanics, Shanghai University, Shanghai 200072, P.R. China

Received 26 May 2005; accepted 8 August 2005
Available online 27 December 2005

Abstract

A new traction boundary integral equation is presented for analyzing the interaction effect of any number of collinear interface cracks in a two-dimensional bimaterial. The dislocation densities on every crack surface are expressed in the products of the characteristic terms and the weight functions, and the unknown weight functions are approximated using the moving least-squares technique based on the constructed orthogonal basis functions. An efficient numerical integral method is employed to evaluate the Cauchy principal integrals that appear in the meshless method. The boundary element-free method is established, and a series of numerical results is presented. The interaction between the collinear interfacial cracks is analyzed.

Keywords: Interface crack; Boundary integral equation; Moving least-squares approximation; Meshless method; Boundary element-free method; Stress intensity factor

1. Introduction

The analysis of interface crack problems is very significant for the study of modern composite structures. Although the stress field around the crack tip has better studied by many researchers [1–6], analytical solutions are not available for collinear interface crack problems with the exception of the case of periodic interface cracks [2]. Systematical numerical results are also difficult to find in the current literatures. A relatively complete work is that of Noda and Oda [7] where the crack opening displacements are expressed as the products of the fundamental density functions and weight functions, and the weight functions are approximated using polynomials. The interaction effect of any number of collinear interface cracks is then numerically analyzed with the hyper-singular integral equations.

Boundary numerical methods, such as the boundary collocation method and the boundary element method, show particular merit in their application to crack problems. In general, the displacement boundary

* Corresponding author. Tel.: +852 3442 6581; fax: +852 2788 7612.
E-mail address: kmliew@cityu.edu.hk (K.M. Liew).

0020-7225/$ - see front matter © 2005 Elsevier Ltd. All rights reserved.
doi:10.1016/j.ijengsci.2005.08.005

integral equation (BIE) can only be used in some simple cases because the geometrical overlapping of the upper and lower surfaces of the crack leads to an indeterminacy of the traditional displacement BIE. Moreover, the kernels of the traction BIE involve hyper-singular terms and the evaluation of singular integrals is arduous. Furthermore, appropriate approaches must also be adopted when the traction BIE is applied to the cracked bodies. For example, in the dual BEM [8,9], the displacement integral equation is applied to the outside boundary and to one side of the crack surface, and the traction integral equation is applied to the other side of the crack surface. Recently, Wang and Chau [10,11] derived a new integral equation for two-dimensional isotropic media by applying integration by parts and other techniques. Although the displacement density and the dislocation density are induced into the equation, the new integral equation seems to be simpler and more complete. In this study, the formulations of Wang and Chau [10,11] are directly employed on a two-dimensional bimaterial with the interface cracks, and a new traction boundary integral equation is obtained.

It is well known that the interfacial crack tip field has an oscillatory character [1–4] which brings a large difficulty to the numerical computation. In many works [12–14], the oscillatory terms are directly neglected. In another works [7,15], researchers express the displacement differences as the products of the fundamental density functions and the weight functions. In this study, the oscillatory character is considered and the similar weight functions that are related to the dislocation densities are approximated using a more flexible and efficient method: the moving least-squares (MLS) approximation.

The MLS approximation is a new technique for modeling unknown variables, and it has some new merits in comparison to other interpolation methods. It has been combined with the finite element method to form meshless methods in many papers, and one review paper [16] provides a good summary. Recently, it has also been combined with the boundary element method [17–19]. In the boundary meshless method, a possible problem is that the singular ill-condition appears in some cases. Another problem arises because the MLS shape functions lack the delta function property of conventional shape functions, and the nodal parameters are not the real nodal quantities of the corresponding variables. Hence, other approaches are needed to impose the boundary conditions [17,18]. Similar to [19], the orthogonal MLS basis is used in this study. This technique directly avoids the appearance of the ill-condition, and it can be better used to the boundary meshless method. Moreover, in the meshless method, the shape functions can only be digitally computed, and a suitable numerical method to evaluate the singular integrals must be employed. We test an efficient method by Torino [20] and use it to evaluate the Cauchy singular integrals.

The main purpose of this paper is to present a more efficient and precise method with which to analyze the interaction between collinear interface cracks. A series of numerical results are given, and some significant phenomena are discussed. The results should provide a valuable reference for the related analyses.

2. Boundary integral equation

Applying integration by parts and some other techniques, Chau and Wang [10] derived a new integral equation for 2-D isotropic media. In this section, that equation is directly employed on a 2-D bimaterial with interface cracks, and a new traction integral equation is obtained.

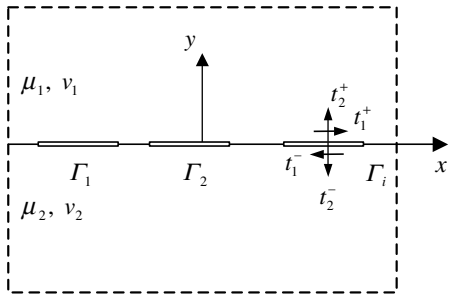

Fig. 1. A set of collinear cracks situated on the interface of a two-dimensional biomaterial; the crack surfaces are applied to arbitrary tractions.

As shown in Fig. 1, we consider two half planes that are perfectly bonded along the interface except for the crack surfaces $\Gamma = \bigcup_{i=1}^{n} \Gamma_i$. Assume that the upper and lower surfaces of the cracks are applied to arbitrary loads. Applying Eq. (20) of Chau and Wang [10] to the upper half plane (noting that no crack is inside the single half plane), we have:

$$\tau(x,+0) = \frac{2}{\pi}\int_{-\infty}^{+\infty} \frac{A_1 u_{,1}(t,+0) - B_1\sigma(t,+0)}{t-x}\,\mathrm{d}t, \tag{1a}$$

$$\sigma(x,+0) = \frac{2}{\pi}\int_{-\infty}^{+\infty} \frac{A_1 v_{,1}(t,+0) + B_1\tau(t,+0)}{t-x}\,\mathrm{d}t. \tag{1b}$$

The Hilbert transform pairs of (1) are [21]:

$$A_1 u_{,1}(x,+0) - B_1\sigma(x,+0) = -\frac{1}{2\pi}\int_{-\infty}^{+\infty} \frac{\tau(t,+0)}{t-x}\,\mathrm{d}t, \tag{2a}$$

$$A_1 v_{,1}(t,+0) + B_1\tau(t,+0) = -\frac{1}{2\pi}\int_{-\infty}^{+\infty} \frac{\sigma(x,+0)}{t-x}\,\mathrm{d}t, \tag{2b}$$

where

$$A_1 = \frac{2\mu_1}{\kappa_1+1}, \quad B_1 = \frac{\kappa_1-1}{2(\kappa_1+1)}, \quad \kappa_1 = \begin{cases} 3-4\nu_1, & \text{for plane strain,} \\ (3-\nu_1)/(1+\nu_1), & \text{for plane stress,} \end{cases}$$

μ_1 is the shear modulus, ν_1 is the Poisson's ratio, σ denotes the normal stress, τ denotes the shear stress, and $u_{,1} = \partial u/\partial x$, $v_{,1} = \partial v/\partial x$ are the displacement densities.

Similarly, for the lower half plane, we have

$$\tau(x,-0) = \frac{2}{\pi}\int_{-\infty}^{+\infty} \frac{A_2 u_{,1}(t,-0) - B_2\sigma(t,-0)}{t-x}\,\mathrm{d}t, \tag{3a}$$

$$\sigma(x,-0) = \frac{2}{\pi}\int_{-\infty}^{+\infty} \frac{A_2 v_{,1}(t,-0) + B_2\tau(t,-0)}{t-x}\,\mathrm{d}t, \tag{3b}$$

and

$$A_2 u_{,1}(x,-0) - B_2\sigma(x,-0) = -\frac{1}{2\pi}\int_{-\infty}^{+\infty} \frac{\tau(t,-0)}{t-x}\,\mathrm{d}t, \tag{4a}$$

$$A_2 v_{,1}(x,-0) + B_2\sigma(x,-0) = -\frac{1}{2\pi}\int_{-\infty}^{+\infty} \frac{\sigma(t,-0)}{t-x}\,\mathrm{d}t, \tag{4b}$$

where

$$A_2 = \frac{2\mu_2}{\kappa_2+1}, \quad B_2 = \frac{\kappa_2-1}{2(\kappa_2+1)}, \quad \kappa_2 = \begin{cases} 3-4\nu_2, & \text{for plane strain,} \\ (3-\nu_2)/(1+\nu_2), & \text{for plane stress.} \end{cases}$$

Along the interface, the continuous conditions are

$$\begin{aligned} &u(x,+0) = u(x,-0) = u(x), \quad v(x,+0) = v(x,-0) = v(x), \\ &\sigma(x,+0) = \sigma(x,-0) = \sigma(x), \quad \tau(x,+0) = \tau(x,-0) = \tau(x), \qquad x \notin \Gamma. \end{aligned} \tag{5}$$

Letting Eqs. (1)–(4) satisfy the continuous conditions (5), and noticing the relationship

$$t_1^{\pm}(x) = \mp\tau(x,\pm 0), \quad t_2^{\pm}(x) = \mp\sigma(x,\pm 0), \qquad x \in \Gamma, \tag{6}$$

we can obtain the following integral equations by algebraic operations:

$$\frac{1}{2\pi}\int_{\Gamma}\frac{(A_1+A_2)\Delta u_{,1}(t)+(B_1+B_2)\sum t_2(t)}{t-x}\,\mathrm{d}t+\frac{\mu_2(\kappa_1-1)-\mu_1(\kappa_2-1)}{\mu_2(\kappa_1+1)+\mu_1(\kappa_2+1)}\times\frac{1}{2}\left[(A_1+A_2)\Delta v_{,1}(x)-(B_1+B_2)\sum t_1(x)\right]=-\frac{2(\mu_1+\mu_2\kappa_1)}{\mu_2(\kappa_1+1)+\mu_1(\kappa_2+1)}\frac{(\mu_2+\mu_1\kappa_2)}{4\mu_1\mu_2}[A_2t_1^+(x)-\mathrm{i}A_1t_1^-(x)], \tag{7a}$$

$$-\frac{1}{2\pi}\int_{\Gamma}\frac{(A_1+A_2)\Delta v_{,1}(t)-(B_1+B_2)\sum t_1(t)}{t-x}\,\mathrm{d}t+\frac{\mu_2(\kappa_1-1)-\mu_1(\kappa_2-1)}{\mu_2(\kappa_1+1)+\mu_1(\kappa_2+1)}\times\frac{1}{2}\left[(A_1+A_2)\Delta u_{,1}(x)+(B_1+B_2)\sum t_2(x)\right]=\frac{2(\mu_1+\mu_2\kappa_1)}{\mu_2(\kappa_1+1)+\mu_1(\kappa_2+1)}\frac{(\mu_2+\mu_1\kappa_2)}{4\mu_1\mu_2}[A_2t_2^+(x)-\mathrm{i}A_1t_1^-(x)], \tag{7b}$$

where $\Delta u_{,1}(x)=u_{,1}(x,+0)-u_{,1}(x,-0)$, $\Delta v_{,1}(x)=v_{,1}(x,+0)-v_{,1}(x,-0)$ are the dislocation densities, and $\sum t_k(x)=t_k^+(x)+t_k^-(x)$ $(k=1,2)$.

To ensure that the displacements are single-valued, the following conditions are necessary:

$$\int_{\Gamma_i}u_{,1}\,\mathrm{d}x=0,\quad \int_{\Gamma_i}v_{,1}\,\mathrm{d}x=0\qquad (i=1,2,\ldots,n). \tag{8}$$

The basic unknowns in (7) are dislocation densities $\Delta u_{,1}$ and $\Delta v_{,1}$, and the upper and lower surface of the crack do not have to be considered separately when (7) is used. In addition, only the singularity in the order $1/r$ is involved in the integral kernels, and no hyper-singularity appears. Another advantage of this equation, as compared to Comninou's equations [5], is that (7) is also effective for the non-symmetric loading. In the following sections, we will establish a meshless numerical scheme based on (7).

3. Moving least-squares approximation for the unknowns

The modeling of the oscillatory character around the interface crack tip is difficult in the boundary element method [22], and many researchers directly neglect the oscillatory terms in their numerical computations [12–14]. The dislocation density for the single interface crack under the uniform tension can be analytically obtained [23,24], and the dislocation densities $\partial\Delta u/\partial x$ and $\partial\Delta v/\partial x$ possess the character $r^{-1/2+\mathrm{i}\varepsilon}$ around the crack tip. Similar to the analysis that is based on the crack opening displacements [5,12–14], the dislocation densities can be expressed in the following form for every crack:

$$\partial\Delta u/\partial x+\mathrm{i}\partial\Delta v/\partial x=(c_i^2-\xi_i^2)^{-1/2}\left(\frac{c_i-\xi_i}{c_i+\xi_i}\right)^{i\varepsilon}[F_{1i}(\xi_i)+\mathrm{i}F_{2i}(\xi_i)], \tag{9}$$

where ε is the bi-constant denoted as

$$\varepsilon=\frac{1}{2\pi}\ln\frac{\mu_1+\mu_2k_1}{\mu_2+\mu_1k_2}, \tag{10}$$

c_i is the length of the ith crack, and $\xi_i=x-x_{0i}$ with x_{0i} corresponding to the coordinate of the center of the ith crack.

In some works [5,12–14], variables that are similar to $F_{1i}(\xi_i)$ and $F_{2i}(\xi_i)$ are approximated by polynomials. Apparently, the ability of polynomial approximation is very limited, and cannot give good results for variables with drastic variation. In addition, the local numerical computation that is associated with polynomial interpolation is quite expensive. Here we attempt to approximate $F_{1i}(\xi_i)$ and $F_{2i}(\xi_i)$ using the MLS technique. The MLS approximation is a new flexible interpolation and has local and global interpolation characteristics, thus the local numerical computation can be easily performed.

The MLS approximation is summarized here, the related details can be found in a review paper by Belytschko et al. [16]. In the MLS approximation, the trail function is

$$F^h(\mathbf{x}) = \sum_{i=1}^{m} p_i(\mathbf{x}) a_i(\mathbf{x}) = \mathbf{p}^{\mathrm{T}}(\mathbf{x})\mathbf{a}(\mathbf{x}), \tag{11}$$

where $p_i(\mathbf{x})$, $i = 1, 2, \ldots, m$, are monomial basis functions, m is the number of terms in the basis, and $a_i(\mathbf{x})$ are the coefficients of the basis functions. Examples of commonly used bases are the linear basis

$$\mathbf{p}^{\mathrm{T}} = (1, x) \text{ in 1D} \quad \text{and} \quad \mathbf{p}^{\mathrm{T}} = (1, x, y) \text{ in 2D}, \tag{12}$$

and the quadratic basis

$$\mathbf{p}^{\mathrm{T}} = (1, x, x^2) \text{ in 1D} \quad \text{and} \quad \mathbf{p}^{\mathrm{T}} = (1, x, y, x^2, xy, y^2) \text{ in 2D}. \tag{13}$$

The unknown coefficients $a_i(\mathbf{x})$ in (11) can be determined by minimizing the weighted discrete L_2 norm

$$J = \sum_{I}^{N} w(\mathbf{x} - \mathbf{x}_I)[\mathbf{P}^{\mathrm{T}}(\mathbf{x}_I)\mathbf{a}(\mathbf{x}_I) - F_I]^2, \tag{14}$$

where $w(\mathbf{x} - \mathbf{x}_I)$ is the weight function with compact support, N is the number of nodes with $w(\mathbf{x} - \mathbf{x}_I) > 0$, and F_I is the nodal parameter. The minimum of J in Eq. (14) with respect to $\mathbf{a}(\mathbf{x})$ leads to a set of linear equations

$$\mathbf{A}(\mathbf{x})\mathbf{a}(\mathbf{x}) = \mathbf{B}(\mathbf{x})\mathbf{F}, \tag{15}$$

where

$$\mathbf{A}(\mathbf{x}) = \sum_{I}^{N} w(\mathbf{x} - \mathbf{x}_I)\mathbf{p}(\mathbf{x}_I)\mathbf{p}^{\mathrm{T}}(\mathbf{x}_I), \tag{16}$$

and

$$\mathbf{B}(\mathbf{x}) = [w(\mathbf{x} - \mathbf{x}_1)\mathbf{p}(\mathbf{x}_1), w(\mathbf{x} - \mathbf{x}_2)\mathbf{p}(\mathbf{x}_2), \ldots, w(\mathbf{x} - \mathbf{x}_N)\mathbf{p}(\mathbf{x}_N)]. \tag{17}$$

Thus, the unknown coefficients $\mathbf{a}(\mathbf{x})$ can be obtained from (15) as

$$\mathbf{a}(\mathbf{x}) = \mathbf{A}^{-1}(\mathbf{x})\mathbf{B}(\mathbf{x})\mathbf{F}. \tag{18}$$

Substituting (18) into (11), the MLS approximation can be written in a standard form as

$$F^h(\mathbf{x}) = \sum_{I=1}^{N} N_I(\mathbf{x}) F_I, \tag{19}$$

where the MLS shape function $N_I(\mathbf{x})$ is defined as

$$N_I(\mathbf{x}) = \sum_{i=1}^{m} p_i(\mathbf{x})[\mathbf{A}^{-1}(\mathbf{x})\mathbf{B}(\mathbf{x})]_{iI} = \mathbf{p}^{\mathrm{T}}(\mathbf{x})\mathbf{A}^{-1}(\mathbf{x})\mathbf{B}_I(\mathbf{x}) \tag{20}$$

with

$$\mathbf{B}_I(\mathbf{x}) = w(\mathbf{x} - \mathbf{x}_I)\mathbf{p}(\mathbf{x}_I). \tag{21}$$

During the MLS approximation, the method may fail because the matrix $\mathbf{A}(\mathbf{x})$ becomes singular in some cases. In the addition, the MLS shape function $N_I(\mathbf{x})$ lacks the delta function property, i.e.

$$N_I(x_j) \neq \delta_{ij}. \tag{22}$$

Hence, the nodal parameters are not the real nodal quantities of the corresponding variables. This complicates the imposition of essential boundary conditions. In the boundary node method [17,18], additional equations are added to impose the boundary conditions which is more computationally expensive than the conventional BEM. Recently, Kitipornchai et al. [19] used the constructed orthogonal MLS basis functions to avoid the appearance of the singular matrix $\mathbf{A}(\mathbf{x})$. It can be used to improve boundary meshless methods. The orthogonal basis function set can be formed as [19]:

$$p_1 = 1,$$

$$p_i = r^{i-1} - \sum_{k=1}^{i-1} \frac{(r^{i-1}, p_k)}{(p_k, p_k)} p_k, \quad i = 2, 3, \ldots, \tag{23}$$

where the inner product (f, g) is denoted as

$$(f, g) = \sum_{i=1}^{N} w(\mathbf{x} - \mathbf{x}_I) f(\mathbf{x}_I) g(\mathbf{x}_I). \tag{24}$$

In Eq. (23), r can be chosen as $\sqrt{x^2 + y^2}$ or $x + y$ for 2D problems and $|x|$ or x for 1D problems.

In this study, the improved MLS method [19] is used to approximate the variables $F_{1i}(\xi_i)$ and $F_{2i}(\xi_i)$ in (10), and the weight function is chosen as [19]

$$w(d) = \begin{cases} \frac{2}{3} - 4d^2 + 4d^3, & d \leqslant \frac{1}{2}, \\ \frac{4}{3} + 4d + 4d^2 - \frac{4}{3}d^3, & \frac{1}{2} < d \leqslant 1, \\ 0, & d > 1. \end{cases} \tag{25}$$

The compact support domain of the evaluation point is determined by choosing the suitable quantity R_0 in the formula

$$d = |x - x_0|/R_0, \tag{26}$$

where x_0 is the coordinate of the evaluation point.

4. Boundary element-free method

To carry out the numerical integration, each crack surface is separated into a series of sub-domains that are called as "integral cells" in some papers [17,18]. The integrals in (7) then become the integrals about the cells.

Some nodes are selected on each cell. The choice of the nodes is independent of the cells, but every cell must contain enough nodes to ensure that the compact support domains cover the whole crack surface.

From the MLS approximation (19), we let

$$F_{1i}(\xi_i) = \sum_{I=1}^{n_I} N_I(\xi_i) F_{1I}, \tag{27a}$$

$$F_{2i}(\xi_i) = \sum_{I=1}^{n_I} N_I(\xi_i) F_{2I}, \tag{27b}$$

where n_I is the number of nodes in which the compact support domains cover the considered field point. The quantities of dislocation densities on any point can then be given by substituting (27) into (9), and the integrals in (7) can be evaluated in the pure numerical scheme.

The source point is chosen as the midpoint between any two adjacent nodes in turn. The integrals are performed on every cell, and $2M$ linear equations can be obtained for a crack that contains $M + 1$ nodes. To solve the problem, the single-value condition of displacements (8) is also discretized on each crack surface. The solution of the equation system directly gives the quantities of $F_1(\xi_i)$ and $F_2(\xi_i)$ for every node, and the stress intensity factors—the items of interest in fracture mechanics—can be calculated from $F_1(\xi_i)$ and $F_2(\xi_i)$.

There are some distinctions between the various definitions of the stress intensity factors of interface crack problems [6,24]. Here, we refer to the Erdogen's definition [4,7,24], and the stress intensity factors can be given in the forms [23,24]

$$K_{\mathrm{I}} + \mathrm{i}K_{\mathrm{II}} = \pm \frac{\sqrt{2\pi}\mu_1\mu_2}{(\cosh \pi\varepsilon)^2} \frac{\mu_1(k_2 + 1) + \mu_2(k_1 + 1)}{(\mu_1 + \mu_2 k_1)(\mu_2 + \mu_1 k_2)} \lim_{r \to 0} \left[\left(\frac{r}{2c_i} \right)^{\frac{1}{2} \pm \mathrm{i}\varepsilon} (\Delta v_{,1} + \mathrm{i}\Delta u_{,1}) \right], \tag{28}$$

where r is the distance measured from the crack tip. Substituting (9) into (28), the stress intensity factors can be calculated as

$$K_{\mathrm{I}} + \mathrm{i}K_{\mathrm{II}} = \pm \frac{\sqrt{\pi/c_i}\mu_1\mu_2}{(\cosh \pi\varepsilon)^2} \frac{\mu_1(k_2+1)+\mu_2(k_1+1)}{(\mu_1+\mu_2 k_1)(\mu_2+\mu_1 k_2)} (F_{1i}(\mp c_i) + \mathrm{i}F_{2i}(\mp c_i)). \tag{29}$$

In Eqs. (28) and (29), the symbols "−" and "+" correspond to the left and right tips of the crack, respectively.

This method sidesteps a troublesome problem: the modeling of the crack tip elements that is associated with BEM in which the chosen modeling method always has a larger effect on the final result.

5. The numerical evaluation of the singular integral

When the source point is located inside an integral cell, the kernel of (7) leads to the singular integrals in the order $1/r$. Generally, the Cauchy singular integral can be analytically or semi-analytically computed in BEM. However, the shape functions are always digitally known in the meshless methods, so the singular integrals must be evaluated in the pure numerical scheme. Researchers have proposed many numerical methods to evaluate Cauchy principal integrals [20,25–27]. We find that the Torino method [20] is very effective for meshless methods. It can be described as follows.

As shown in Fig. 2, the singular pole t is located on the integral interval from a to b (assuming that point t is nearer to b than to a). First, a suitable point c is selected so that point t is equally near to c and b. $2m$-point Gauss ruler points are used on the segments from a to c and from c to b, and then the whole integral can be evaluated with the degree of exactness $4m$ as

$$\mathbf{P}\int_a^b \frac{f(x)}{x-t}\,\mathrm{d}x = \int_a^c \frac{f(x)}{x-t}\,\mathrm{d}t + \mathbf{P}\int_c^b \frac{f(x)}{x-t}\,\mathrm{d}x = A_0^{(1)} f(t) + \sum_{i=1}^{2m}[A_i^{(1)} f(x_i) + A_i^{(2)} f(y_i)] + R_{(2m)}^{(2)}(f), \tag{30}$$

where

$$\begin{aligned} &x_i = (c-a)\xi_i/2 + (a+c)/2, \quad y_i = (b-c)\xi_i/2 + (b+c)/2,\\ &A_i^{(1)} = (c-a)H_i/2(x_i - t), \quad A_i^{(2)} = (b-c)H_i/2(y_i - t),\\ &A_0^{(1)} = \ln\left|\frac{c-t}{a-t}\right| - \sum_{i=1}^{2m} A_i^{(1)}, \end{aligned} \tag{31}$$

with ξ_i and H_i being the Gauss quadrature point and weight respectively.

Moreover, the integral appears in the singularity in the order $1/\sqrt{r}$ on the crack tips for the crack tip cells. The transform $s = \sqrt{a_i \pm \xi_i}$ can be introduced to eliminate this singularity, and the integrals then become the general integrals or Cauchy principal integrals.

6. Numerical results

Noda and Oda have obtained some numerical results for various elastic constants [7]. Noting that the stress intensity factors only depend on the bi-constant ε, we discuss the effect of the bimaterial on the stress intensity factors only by varying the bi-constant. The bimaterial is subjected to uniform remote tension σ_y^{∞} in the y-direction (see Figs. 3 and 7). In addition, to hold the condition of continuity of stress and displacement along the interface, it is necessary that the remote stresses $\sigma_{x,1}^{\infty}$ and $\sigma_{x,2}^{\infty}$ in the x-direction follow the relation [2]

$$\sigma_{x,2}^{\infty} = \frac{1}{1+k_2}\left[\frac{\mu_1}{\mu_2}(1+k_1)\sigma_{x,1}^{\infty} + \left\{3 - k_2 - \frac{\mu_2}{\mu_1}(3-k_1)\right\}\sigma_y^{\infty}\right]. \tag{32}$$

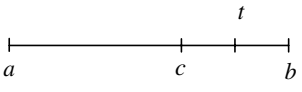

Fig. 2. The integral interval is divided into two segments for the evaluation of singular integrals.

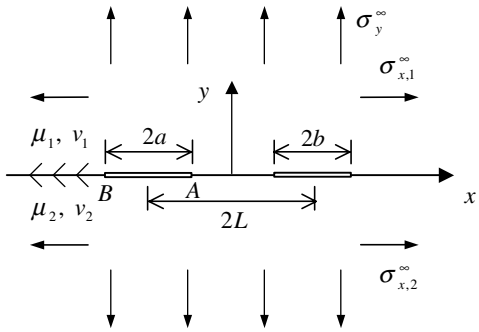

Fig. 3. Two collinear interface cracks in a bimaterial that are subjected to remote uniform tension stress.

6.1. Two collinear cracks and the convergence of the results

To test the efficiency of our method, we firstly consider the case of two interface cracks with the same length (letting $a = b$ in Fig. 3). The distance between the centers of the two cracks is fixed as $L = 3a$. Fifteen integral cells are uniformly selected on each crack surface. Table 1 shows the results for crack tips A and B by varying

Table 1
Fifteen integral cells are uniformly selected and M nodes are uniformly used on each crack surface

M	$\varepsilon = 0$		$\varepsilon = 0.1$			
	Y_{IA}	Y_{IB}	Y_{IA}	Y_{IIA}	Y_{IB}	Y_{IIB}
10	1.11231	1.05169	1.05890	0.22693	1.00366	0.19442
15	1.11243	1.05168	1.05912	0.22721	1.00378	0.19460
20	1.11244	1.05167	1.05926	0.22736	1.00390	0.19473
25	1.11246	1.05168	1.05939	0.22747	1.00402	0.19482
30	1.11247	1.05168	1.05798	0.22592	1.00262	0.19338
35	1.11262	1.05183	1.05816	0.22606	1.00284	0.19351
40	1.11245	1.05166	1.05789	0.22582	1.00258	0.19329
Ana [28]	1.11247	1.05168				

The normalized stress intensity factors $Y_{I,II} = K_{I,II}/\sigma_y^\infty\sqrt{\pi a}$ for two collinear cracks (Fig. 3).

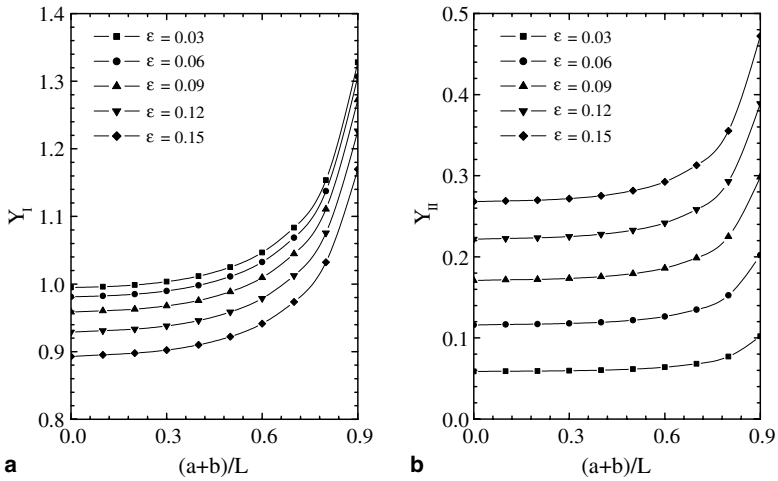

Fig. 4. The normalized stress intensity factors versus $(a + b)/L$ for different values of ε. The ratio of the lengths of two cracks is fixed as $b/a = 0.6$. (a) $Y_I = K_I/\sigma_y^\infty\sqrt{\pi a}$, (b) $Y_{II} = K_{II}/\sigma_y^\infty\sqrt{\pi a}$.

the number of nodes chosen on the crack surface. M denotes the number of nodes on the single crack, and the normalized stress intensity factors are defined as $Y_{\mathrm{I,II}} = K_{\mathrm{I,II}}/\sigma_y^{\infty}\sqrt{\pi a}$. When $\varepsilon = 0$, the problem corresponds to the homogeneous case, and the analytical solution can be found in the handbook [28]. In this test, R_0 in Eq. (26) is properly chosen so that 4–6 nodes are involved in the support domain of any evaluation point. In Table 1, the results are very close when the number of nodes is larger than 15. However, unlike in BEM and FEM, we cannot find a distinct uniform convergence, and this is a natural phenomenon associated with meshless methods.

Two cracks with different lengths (Fig. 3) are also calculated. The maximum mode I and II stress intensity factors always occur at the inner tip of the longer crack. In Figs. 4 and 5, the ratio b/a of the lengths of two cracks is fixed as 0.6 and 0.3, and the normalized stress intensity factors for the inner tip (i.e. the tip A) of the longer crack are plotted as the function of the distance between the centers of the two cracks. In Fig. 6, the distance between the centers of the two cracks is fixed as $2.5a$, and the normalized stress intensity factors are plotted as the function of the ratio of the lengths of two cracks.

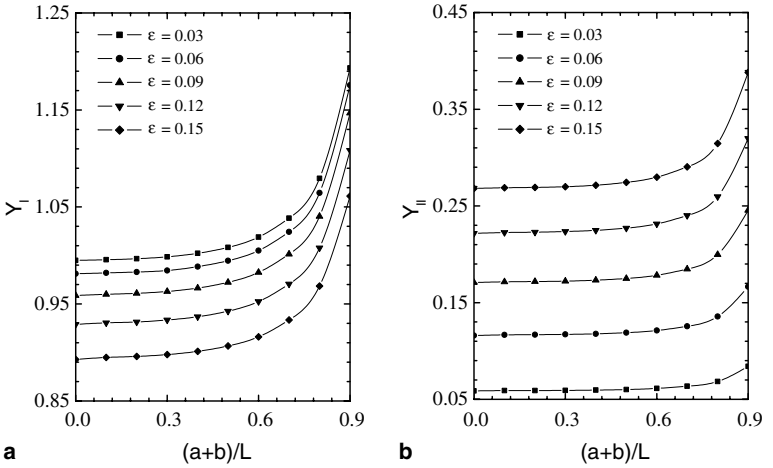

Fig. 5. The normalized stress intensity factors versus $(a + b)/L$ for different values of ε. The ratio of the lengths of two cracks is fixed as $b/a = 0.3$. (a) $Y_{\mathrm{I}} = K_{\mathrm{I}}/\sigma_y^{\infty}\sqrt{\pi a}$, (b) $Y_{\mathrm{II}} = K_{\mathrm{II}}/\sigma_y^{\infty}\sqrt{\pi a}$.

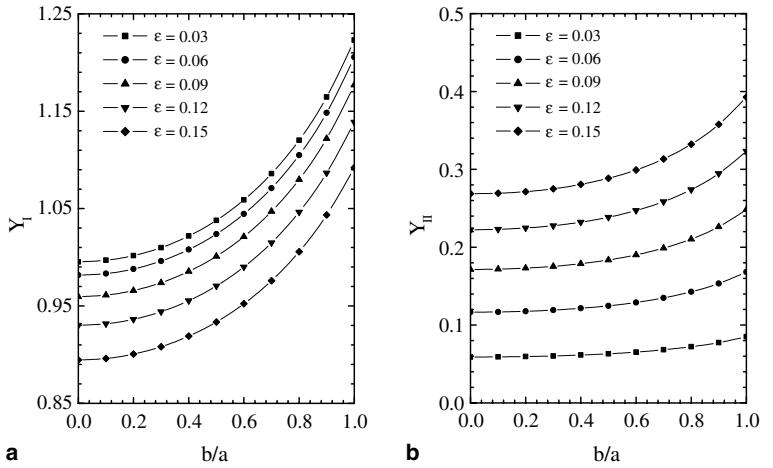

Fig. 6. The normalized stress intensity factors versus b/a for different values of ε. The distance between the centers of two cracks is fixed as $2.5a$. (a) $Y_{\mathrm{I}} = K_{\mathrm{I}}/\sigma_y^{\infty}\sqrt{\pi a}$, (b) $Y_{\mathrm{II}} = K_{\mathrm{II}}/\sigma_y^{\infty}\sqrt{\pi a}$.

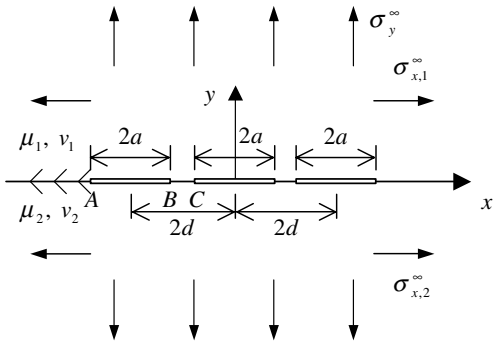

Fig. 7. Three collinear interface cracks with the same length and the equal interval in a bimaterial that is subjected to remote uniform tension stress.

6.2. Three collinear cracks

The numerical results for three collinear cracks with the same length and equal interval (see Fig. 7) are listed in Table 2. The analytical solutions for the homogeneous case ($\varepsilon = 0$) are from the handbook [28], and it can be seen that our numerical results are very close to the analytical results even when $a/d = 0.9$ (i.e. the cracks are very close). The maximum mode I stress intensity factor always appears on the middle crack, but the maximum mode II stress intensity factor is associated with the middle crack for the small value of a/d and with the outer crack for the large value of a/d.

Table 2
The normalized stress intensity factors $Y_{\mathrm{I,II}} = K_{\mathrm{I,II}}/\sigma_y^\infty\sqrt{\pi a}$ for different ε and a/d

		a/d								
ε		0.1	0.2	0.3	0.4	0.5	0.6	0.7	0.8	0.9
0	Y_{IA}	1.00148	1.00583	1.01294	1.02295	1.03629	1.05381	1.07722	1.11030	1.16437
	Ana [28]	1.00150	1.00585	1.01296	1.02298	1.03631	1.05383	1.07724	1.11032	1.16439
	Y_{IB}	1.00263	1.00700	1.01708	1.03351	1.05911	1.09913	1.16454	1.28344	1.56419
	Ana [28]	1.00165	1.00702	1.01710	1.03353	1.05913	1.09915	1.16456	1.28348	1.56454
	Y_{IC}	1.00250	1.01028	1.02405	1.04527	1.07661	1.12314	1.19555	1.32132	1.60651
	Ana [28]	1.00252	1.01030	1.02407	1.04529	1.07663	1.12316	1.19558	1.32136	1.60685
0.03	Y_{IA}	0.99686	1.00121	1.00832	1.01833	1.03168	1.04921	1.07264	1.10577	1.15991
	Y_{IIA}	0.05911	0.05932	0.05962	0.05997	0.06035	0.06071	0.06101	0.06114	0.06081
	Y_{IB}	0.99700	1.00237	1.01243	1.02881	1.05433	1.09418	1.15923	1.27730	1.55528
	Y_{IIB}	0.05913	0.05950	0.06052	0.06167	0.06406	0.06817	0.07561	0.09082	0.13241
	Y_{IC}	0.99788	1.00565	1.01940	1.04058	1.07185	1.11824	1.19037	1.31547	1.59850
	Y_{IIC}	0.05917	0.05965	0.06052	0.06194	0.06421	0.06791	0.07436	0.08719	0.12186
0.09	Y_{IA}	0.96117	0.96550	0.97261	0.98265	0.99605	1.01371	1.03735	1.07081	1.12549
	Y_{IIA}	0.17173	0.17237	0.17327	0.17433	0.17546	0.17654	0.17743	0.17781	0.17681
	Y_{IB}	0.96131	0.96660	0.97648	0.99251	1.01734	1.05584	1.11811	1.22959	1.48576
	Y_{IIB}	0.17180	0.17292	0.17524	0.17940	0.18650	0.19872	0.22081	0.26573	0.38764
	Y_{IC}	0.96218	0.96987	0.98347	1.00436	1.03507	1.08036	1.15025	1.27009	1.53617
	Y_{IIC}	0.17194	0.17335	0.17595	0.18019	0.18694	0.19794	0.21704	0.25491	0.35660
0.15	Y_{IA}	0.89610	0.90040	0.90750	0.91759	0.93113	0.94904	0.97310	1.00724	1.06297
	Y_{IIA}	0.26907	0.27012	0.27161	0.27336	0.27523	0.31205	0.27804	0.27908	0.27733
	Y_{IB}	0.89621	0.90137	0.91691	0.92625	0.94973	0.98560	1.04243	1.14104	1.35519
	Y_{IIB}	0.26918	0.27103	0.27486	0.28170	0.29337	0.31338	0.34936	0.42195	0.61584
	Y_{IC}	0.89708	0.90464	0.91794	0.93826	0.96787	1.01105	1.07659	1.18631	1.42000
	Y_{IIC}	0.26940	0.27173	0.27602	0.28300	0.29408	0.31205	0.34309	0.40417	0.56621

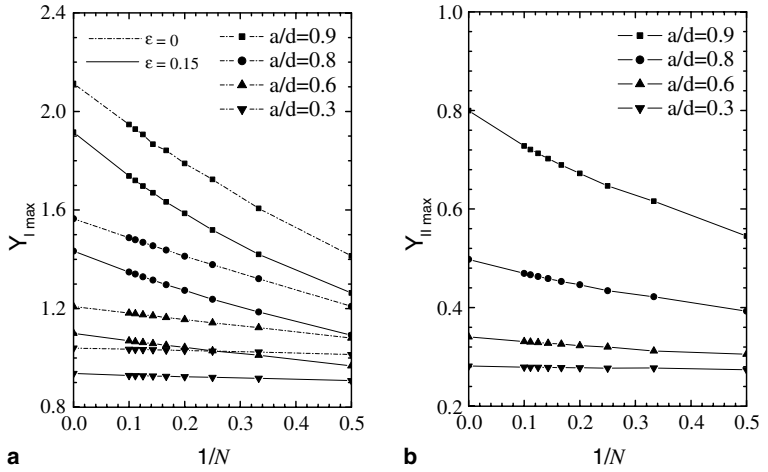

Fig. 8. The maximum normalized stress intensity factors versus the reciprocal of the number of the interface cracks; the distance of the center of any two adjacent cracks is fixed as $3a$ (referring Fig. 7, $d = 3a$). (a) $Y_{\mathrm{I}_{\max}} = K_{\mathrm{I}_{\max}}/\sigma_y^{\infty}\sqrt{\pi a}$; (b) $Y_{\mathrm{II}_{\max}} = K_{\mathrm{II}_{\max}}/\sigma_y^{\infty}\sqrt{\pi a}$.

6.3. Any number of collinear cracks

After the programs for two and three collinear cracks are completed, the program for the case of any number of collinear cracks is easily produced. Any number of collinear cracks with the same length and equal interval are also analyzed by Noda and Oda [7], who significantly find that the maximum mode I stress intensity factor has an approximately linear relation with the reciprocal of the number of interface cracks. Our computation gives a similar result for the mode I and II stress intensity factors. In Fig. 8, the crack interval is fixed as $3a$ (referring to Fig. 7, $d = 3a$), and the obtained discrete dots are nearly on the same straight line. The extrapolated limiting values for $N \to \infty$ are close to the analytical values [23,29] for the periodic interface cracks. Hence, the maximum stress intensity factors for any number of cracks can approximately be determined from Fig. 8. In addition, the maximum mode I stress intensity factor appears at the middle crack (for the number of the cracks being odd) or the middle two cracks (when the number of cracks is even), but the maximum mode II stress intensity factor is general associated with the crack that is closest to the middle crack.

7. Conclusions

The proposed traction boundary integral equation can be used to efficiently analyze the bimaterial with interfacial cracks. The MLS approximation is employed to approximate the unknown weight functions, and good results can be obtained even when the cracks are very close. This study shows that the MLS approximation is a flexible interpolation method and can be better used to model variables that are, as a whole, difficult to be modeled with other methods. A numerical method is adopted to evaluate the Cauchy principal integrals, and this method should also be very efficient for other meshless methods.

The stress intensity factors for the collinear interface cracks are analyzed by varying the bi-constant. The mode I and II stress intensity factors have an approximately linear relation with the reciprocal of the number of the interface cracks, which is very valuable for determining the quantities of the stress intensity factors for any number of collinear interface cracks.

Acknowledgement

The work in this project was fully supported by a grant from the Research Grants Council (RGC) of the Hong Kong Special Administrative Region, China (Project No. CityU 1011/02E).

References

[1] M.L. Williams, The stress around a fault or crack in dissimilar media, Bull. Seismol. Soc. Amer. 49 (1959) 199–204.
[2] J.R. Rice, G.C. Sih, Plane problems of cracks in dissimilar media, J. Appl. Mech. 32 (1965) 418–423.
[3] A.H. England, A crack between dissimilar media, J. Appl. Mech. 32 (1965) 400–402.
[4] F. Erdogan, Stress distribution in bonded dissimilar materials with cracks, J. Appl. Mech. 32 (1965) 403–410.
[5] M. Comninou, The interface crack, J. Appl. Mech. 44 (1977) 631–636.
[6] J.R. Rice, Elastic fracture mechanics concepts for interfacial crack, J. Appl. Mech. 55 (1988) 98–103.
[7] N.A. Noda, K. Oda, Interaction effect of stress intensity factors for any number of collinear interface cracks, Int. J. Fract. 84 (1997) 117–128.
[8] H.K. Hong, J.T. Chen, Derivations of integral-equations of elasticity, J. Eng. Mech.—ASCE 114 (6) (1988) 180–184.
[9] A. Portela, M.H. Aliabadi, D.P. Rooke, The dual boundary element method: effective implementation for crack problems, Int. J. Numer. Meth. Eng. 33 (1992) 1269–1287.
[10] K.T. Chau, Y.B. Wang, A new boundary integral formulation for plane elastic bodies containing cracks and holes, Int. J. Solids Struct. 36 (1999) 2041–2074.
[11] Y.B. Wang, K.T. Chau, A new boundary element for plane elastic problems involving cracks and holes, Int. J. Fract. 89 (1997) 1–20.
[12] E.I. Shifrin, B. Brank, G. Surace, Analytical–numerical solution of elliptical interface crack problem, Int. J. Fract. 94 (3) (1989) 201–215.
[13] M.C. Chen, N.A. Noda, R.J. Tang, Application of finite-part integrals to planar interfacial fracture problems in three-dimensional bimaterials, ASME J. Appl. Mech. 66 (1999) 885–890.
[14] R. Yukki, S.B. Cho, Efficient boundary element analysis of stress intensity factors for interface cracks, Eng. Fract. Mech. 34 (1989) 179–188.
[15] N.A. Noda, M. Kagita, M.C. Chen, K. Oda, Analysis of stress intensity factors of a ring-shaped interface crack, Int. Solids Struct. 40 (2003) 6577–6592.
[16] T. Belytschko, Y. Krongauz, D. Organ, M. Fleming, P. Krysl, Meshless methods: an overview and recent developments, Comput. Meth. Appl. Mech. Eng. 139 (1996) 3–47.
[17] Y.X. Mukherjee, S. Mukherjee, The boundary node method for potential problems, Int. J. Numer. Meth. Eng. 40 (5) (1997) 797–815.
[18] V.S. Kothnur, S. Mukherjee, Y.X. Mukherjee, Two-dimensional linear elasticity by the boundary node method, Int. J. Solids Struct. 36 (8) (1999) 1129–1147.
[19] S. Kitipornchai, K.M. Liew, Y.M. Cheng, A boundary element-free method (BEFM) for three dimensional elasticity problems, Comput. Mech. 36 (2005) 13–20.
[20] G.M. Torino, The numerical evaluation of one-dimensional Cauchy principal value integrals, J. Comput. 29 (1982) 337–354.
[21] A.D. Polyanin, A.V. Manzhirov, Handbook of Integral Equations, CRC Press LLC, Florida, 1998.
[22] C.L. Tan, Y.L. Gao, Treatment of bimaterial interface crack problems using the boundary element method, Eng. Fract. Mech. 36 (6) (1990) 919–932.
[23] Y.B. Wang, A boundary integral equation method of plane problems of interface cracks in elastic bimaterials, J. Lanzhou Univ. (Nat. Sci.) 31 (1) (1995) 14–21.
[24] K.B. Broberg, Cracks and Fracture, Academic Press, California, 1999.
[25] L.M. Delves, The numerical evaluation of principal value integrals, J. Comput. 10 (1968) 389–391.
[26] D. Elliott, D.F. Paget, Gauss type quadrature rules for Cauchy principal value integrals, Math. Comp. 33 (1979) 301–309.
[27] V.J.E. Stark, A generalized quadrature formula for Cauchy integral, AIAA J. 9 (1971) 1854–1855.
[28] H. Tada, P.C. Paris, G.R. Irwin, The Stress Analysis of Cracks Handbook, third ed., Professional Engineering Publishing, London, 2000.
[29] Y. Murakami, Stress Intensity Factors Handbook, vol. 1, Pergamon Press, Oxford, 1987.